Corrosion inhibition of aluminum by coatings formulated with Al-Zn-vanadate hydrotalcite

J.M. Vega, N. Granizo, D. de la Fuente*, J. Simancas and M. Morcillo

Department of Materials Engineering, Degradation and Durability.
National Centre for Metallurgical Research (CENIM/CSIC).
Av. Gregorio del Amo, 8, 28040 Madrid (Spain).

ABSTRACT

The hydrotalcite structure is an ionic lamellar solid with positively charged layers incorporating two kinds of metallic cations and hydrated gallery anions. The ability of these compounds to retain aggressive ions and simultaneously release a corrosion inhibitor is the main reason for the development of hydrotalcite compounds to replace hexavalent chromium compounds (chromates) as inhibitive pigments.

In this study, alkyd coatings formulated with Al-Zn-vanadate hydrotalcite, at different pigment concentrations were applied on aluminum specimens. The painted panels were subjected to different accelerated tests (condensing humidity, salt spray and Kesternich) and atmospheric exposure in atmospheres of different aggressiveness. Corrosion performance was evaluated by Electrochemical Impedance Spectroscopy (EIS). A traditional zinc chromate pigment was also tested for comparative purposes.

The obtained results confirm that hydrotalcite compounds achieve corrosion inhibition of the underlying aluminum substrate. It has been shown that an increase of anticorrosive pigment content (for a constant Pigment Volume Concentration) does not always improve the primer behavior, but a larger amount of vanadates released from Al-Zn-vanadate hydrotalcite particles does improve anticorrosive behavior.

Keywords: Chromate-free coatings, vanadate, aluminum, anion-exchange hydrotalcite, layered double hydroxides (LDHs).

* Corresponding author. Tel.: +34 91 5544506. Fax.: +34 91 5345108
E-mail address: delafuente@cenim.csic.es

1. Introduction

It is known that the combination of a physical barrier, a chemical inhibitor and an electrical resistor improves the performance of coating systems [1]. The role of pigments as anticorrosive inhibitors depends on how they influence the above parameters.

Nowadays there is a special interest to study and develop new anticorrosive pigments to replace chromates (one of the most effective inhibitive pigments) due to their toxicity and carcinogenic effects. The use of ion-exchangeable pigments (IEP) is one alternative that is being studied. Layered double hydroxides (LDHs), also known as hydrotalcite-like compounds (HTlc), are one example of IEPs with the following general equation: $[M^{2+}_{1-x}M^{3+}_{x}(OH)_2]^{x+}(A^{n-}_{x/n})\cdot mH_2O$, where M^{2+} and M^{3+} are the divalent and trivalent metals. Their structure consists of brucite-like layers comprised of edge-sharing $Mg(OH)_6$ octahedra. The isomorphic substitution of Mg^{2+} by M^{3+} generates a positive charge in the hydroxyl sheet. This net positive charge is compensated by anions (usually CO_3^{2-}) and water. In general these compounds consist of a host structure with a fixed charge and within the host there are 'galleries' that can accommodate anions and solvent molecules.

This intrinsic feature allows hydrotalcites (HTs) to be described as anion-exchange compounds. HTs are thus being studied in corrosion research as anticorrosive inhibitors loaded with different anions [2, 3] and also in relation with coating application [4-8]. These pigments are commonly used in the form of solid particulate materials dispersed throughout the paint film. In this case the cathodic, anodic or both reactions are suppressed for as long as the inhibitor is present. The proposed mechanism makes the use of these pigments in coating formulation more attractive, since they can retain aggressive anions (e.g. Cl^-) during their permeation through the paint and at the same time can release a corrosion inhibitor (e.g. vanadate) during the leaching process.

Several studies have been carried out to assess the anticorrosive behavior of different types of coatings (conversion coating, sol-gels, model coatings, commercial primers, etc.) formulated with different HTs [9-23]. Williams and McMurray showed that HT can provide effective inhibition against filiform corrosion propagation on organic-coated AA2024-T3 alloy [9-11]. Alvarez et al. observed by EIS that the addition of HT

to sol-gel films improved the corrosion resistance of coated AA2024-T3 alloy in salt spray [12]. Anticorrosive improvements were studied by the application of a HT conversion coating on AZ91D alloy, AA2024-T3 alloy and galvanized steel. Different corrosion resistance levels and an improvement in the adhesion properties were found [13, 16-21]. On the other hand, Yu et al. observed by EIS some inhibition by adding HT to an epoxy resin applied on AZ31 alloy [14].

Among the different HTs, attention has particularly been paid to Al-Zn-vanadate hydrotalcite (HT-V) [21, 24-27]. With regard to HT-V, Buchheit et al. studied inhibition on AA2024-T3 alloy coated with an epoxy binder formulated with HT-V pigment in salt spray. They found that HT-V affords protection by a combination of barrier protection and active inhibition. Corrosion protection was also observed at scribes, where the underlaying bare metal is exposed [24, 27]. On the other hand, Chico et al. observed a irregular behavior of primers formulated with HT-V and applied on low carbon steel [25]. Zheludkevich et al. studied a commercial water-borne epoxy primer formulated with HT-V on AA2024 alloy. These samples displayed good behavior during immersion in sodium chloride but showed significantly higher blistering in the humidity condensation test compared to chromates [26].

Therefore, the few studies conducted with coatings formulated with HT-V are not conclusive about their anticorrosive efficiency and controversy surrounds their functioning mechanisms in a real commercial primer.

The present work focuses on the study of anticorrosive protection of aluminum by alkyd paint coatings formulated with HT-V, assessing performance in environments with different aggressiveness, both natural and accelerated.

2. Experimental

HT-V pigment was prepared in the laboratory following the coprecipitation method developed by Kooli and Jones [28] and described by Buchheit et al. [27], wherein the HT-V compound is synthesized using decavanadate anions to compensate the positive charge in the HT structure $[Zn_x^{2+}Al_y^{3+}(OH)_{2(x+y)}]^{y+}$, with an x:y ratio of 2:1.

Table 1 shows the composition of the five alkyd paints used in this study. The different paints were formulated maintaining the same pigment volume concentration (PVC). In

order to know the PVC, the HT-V density (ρ) was determined experimentally according to ISO 787-10 by the method of Gay-Lussac [29].

As can be seen in Table 1, a TiO_2 (25%) coating, formulated without anticorrosive pigment, and a $ZnCrO_4$ (10%) coating, with 10% zinc chromate, were also considered as references. HT-V (5%), HT-V (10%) and HT-V (15%) coatings (containing 5%, 10% and 15% HT-V, respectively) were prepared and applied in order to study the effect of the pigment content on anticorrosive behavior. The paints were applied by air-spraying to a dry film thickness of 60 ± 10 µm on degreased 15 x 10 cm panels prepared from 1 mm aluminum 1050 plate. A scribe of 0.3 mm width and 6 cm length was made in the lower part of the panels to evaluate the inhibitive properties of the different pigments in natural and accelerated tests.

Adhesion measurements were carried out on painted panels according to the cross cut test described in ISO 2409:1991 (E) [30].

2.1 Corrosion tests

The paints were subjected to the following accelerated corrosion tests: resistance to condensing humidity (ISO 6270-1) [31], salt spray (ISO 9227) [32] and Kesternich (ISO 3231, 0.2 l SO_2) [33]. An atmospheric corrosion exposure test was also conducted at two test sites: one located on the roof of the CENIM laboratory in Madrid (Spain), in an urban atmosphere of corrosivity category C2-C3, and the other in Aviles (Spain), in an urban-mild industrial atmosphere of corrosivity category C3, according to ISO 9223[34].

2.2 Electrochemical Impedance Spectroscopy (EIS)

The anticorrosive performance of the coatings was investigated by EIS in a classic three-electrode cell consisting of a silver/silver chloride reference electrode, a stainless steel counter electrode and the coated aluminum 1050 specimens as a working electrode in the horizontal position, with a working area of 9.62 cm^2. EIS measurements were carried out at room temperature using a potentiostat/galvanostat (AutoLab EcoChemie PGSTAT30) equipped with a FRA2 frequency response analyzer module. Frequency scans were carried out by applying a ± 5 mV amplitude sinusoidal wave perturbation, close to the corrosion potential. Five impedance sampling points were registered per

decade of frequency. The analyzed frequency range was from 100 kHz to 1 mHz and the electrolyte used was 0.1M sodium sulphate solution. The impedance data was analyzed using the electrochemical impedance software ZView® (Version 3.1c, Scribner Associates, Inc., USA).

Different measurements were carried out. On one hand, the samples exposed to the accelerated tests were evaluated after different exposure times. On the other hand, the samples exposed to the natural atmospheres were evaluated after 1 year of exposure.

3. Results

3.1 Accelerated corrosion tests

Table 2 offers a summary of the results obtained in the accelerated corrosion tests. The evaluation of blistering of the painted surface was performed according to the standard ASTM D714 [35]. Blister size and frequency values have been converted into numerical values using the Keane conversion table [36]. Delamination at the scribe was also evaluated. However, as can be seen in Table 2, great delamination was only observed for the HT-V (15%) primer after 120h of exposure in the Kesternich test, and significantly lower delamination in case of HT-V (10%) in the same accelerated test. The resistance to humidity test has provided the most significant differences, where TiO_2 and HT-V (10%) primers showed the lowest blistering after 300h of exposure. When the exposure time is increased, general blistering can be observed in all cases.

Table 3 shows the R_p values obtained by EIS measurements in the three accelerated tests considered after different exposure times.

3.2 Atmospheric exposure

After one year of atmospheric exposure all the primers showed an excellent condition, with a complete absence of blistering and only slight delamination around the scribe for the HT-V (15%) primer in the Madrid atmosphere.

Nyquist impedance diagrams are shown in Figures 1 and 2. The TiO_2 primer showed the lowest resistance values in both atmospheres. Similar low values where obtained for $ZnCrO_4$ (10%) in Madrid and for HT-V (5%) in Aviles. Better behavior was found for the rest of the primers in both atmospheres. However, one year of atmospheric exposure is not enough time to reach conclusive effects.

4. Discussion

The most widely used equivalent circuit (EC) model for the metal/coating system is shown in Figure 3, where three time constants (τ) can be observed. R_s is the electrolyte resistance; R_i is the electric resistance of the protective coating or also known as pore resistance; C_c is the capacitance of the protective coating; R_{ct} is the charge transfer resistance of the corrosive process; C_{dl} is the double layer capacitance; and Z_w is the Warburg finite diffusion impedance. The parameters R_i and C_c, and their evolution in time supply information on the characteristics of the protective system (coating resistance and capacitance) and on its maintenance or deterioration, while the parameters R_{ct} and C_{dl} yield information on the corrosion processes at the bottom of the pores in the coating, or on all the metallic surface if the coating permeability allows the diffusion of water [37-39].

However, when only one or two time constants can be observed, the EC can be reduced to R_s-R_iC_c or R_s-R_iC_c-$R_{ct}C_{dl}$ respectively, although when exposure time increases, some of this time constant may be poorly defined or overlapping in the impedance diagram. In order to evaluate the corrosion resistance, polarization resistance (R_p) gives an idea about the corrosion rate because it is inversely proportional. R_p is the sum of all the resistances present.

The *condensing humidity test* has revealed the most significant differences between the coatings due to the different resistance to osmotic blistering presented by the considered primers according to the water solubility of the pigments. Blistering may also occur by local alkalization of the metal substrate in the presence of pigments. Blistering has been observed on all the primers, but surprisingly HT-V (10%) does not show a similar or intermediate behavior between the others HT-V primers (Table 2) but a significantly lower osmotic blistering. The R_p values obtained by EIS (Table 3) normally increase with exposure time. The metal surface is being corroded and the formed corrosion products and the blisters are increasing the total resistance in the impedance diagram. Figure 4 shows the Bode plots obtained after 168h of exposure, although this behavior is maintained for a longer time. A single time constant can be observed in three of the primers, HT-V (10%), TiO_2 and $ZnCrO_4$, but three time constants are present for HT-V (5%) and HT-V (15%). This result may indicate the presence of more defects on these primers and could be one reason for the premature blistering encountered (Table 2).

Blistering in the humidity test was previously reported on a water-base epoxy coating formulated with a fixed quantity of HT-V pigment [26].

Finally, it is interesting to point out that $ZnCrO_4$ (10%) and HT-V (10%) primers have the highest and the lowest R_p values, respectively, after 168 and 816h. One possible explanation for the low Rp value offered by the HT-V (10%) could be the low blistering shown by this primer. Water takes longer to get the metal/paint interface and to start the corrosion process. Additionally, although the adhesion of all HT-V primers to the metallic substrate was generally poor, the HT-V (10%) showed the best behavior (Figure 5). Similar results were previously reported on steel substrates [40].

With regard to the *salt spray test*, Figure 6 shows a single time constant and a high impedance modulus for all the primers after 576h, although HT-V (5%) and HT-V (15%) show the lowest resistance values. This may again indicate the presence of defects on these primers that could enhance the permeability of aggressive anions. The R_p values obtained in the salt spray test follow the same trend seen in the condensing humidity test, with an increase in resistance with exposure time (Table 3). The final resistance is one or even two orders of magnitude higher for all the primers compared to the values obtained in the humidity test. On the other hand, blistering is almost negligible in all the specimens (Table 2). These differences may indicate the metal/interface stability and may also be a sign of the difficulty for Cl^- to initiate local corrosion over the metal, due to the low permeability rate of this aggressive anion in all the studied primers [41].

Finally, the samples were also exposed to a simulated industrial atmosphere following the *Kesternich test*. The resistance values after 672h of exposure are high for all the primers formulated with anticorrosive pigments. However the TiO_2 primer show less resistance, around two-three orders of magnitude lower, compared to any coating with anticorrosive pigment (Table 3). When exposure time increases (1008h), the R_p decreases for all the HT-V primers, remains constant for $ZnCrO_4$, and increases 20 times for the TiO_2 primer. Figure 7 shows the Bode plots after 1008h of exposure to the Kesternich test. Two time constants and worse behavior were observed for all the primers compared to $ZnCrO_4$ (10%), which showed only one single time constant. This may be due to the presence of defects and a lower inhibitor power of these primers compared to $ZnCrO_4$ in this very aggressive environment.

Therefore, some evidence of a certain inhibition capacity of HT-V compared with TiO_2 was observed in the accelerated corrosion tests, although the chromate primers still behave better. This active corrosion protection may be originated by the release of vanadates from the pigment. The simultaneous release of Zn^{2+} observed by other authors may also improve the corrosion resistance [27]. The poor performance shown by the HT-V (15%) primer could be due to adhesion failure at the metal/paint interface (Figures 5 and 8).

The results obtained in the natural exposure test will be discussed from the Nyquist plots. According to the proposed EC, the low-frequency arc in the Nyquist plot is related to the double layer capacitance and charge-transfer at the pore base of the paint system and/or with mass transport processes occurring within the pores, whilst the arc appearing at high frequencies is related to the paint coating itself. In the case of Figures 1 and 2, a single time constant can be observed in almost all the primers, although a second time constant starts to appear in some of them. The arcs in Figure 1 for TiO_2 and $ZnCrO_4$ (10%) primers exposed to the Madrid atmosphere indicate lower impedance for those coatings, with phase angles of -12 θ and -9 θ, respectively (Table 4). This means more resistive behavior than the other primers and is a clear indication that the corrosion process may be initiated earlier.

On the other hand, the TiO_2 and HT-V (5%) primers showed the lowest impedance values after one year exposure to the Aviles atmosphere (Figure 2). However, the phase angle values were -17 θ and -35 θ, respectively. This difference shows that HT-V (5%) still has some capacitive component compared with TiO_2, despite the other HT-V primers behaving better in this atmosphere. Although there are some differences between the primers, all of them show low capacitance values (Table 4).

In summary, HT-V (10%) primer has shown more corrosion protection than the other HT-V primers. 5% of HT-V pigment may not be enough inhibitor in the coating if it is assumed that this anticorrosive compound provides active inhibition and barrier properties, as observed in the epoxy coatings [24]. On the other hand, the HT-V (15%) primer has shown good behavior in natural testing but not in the accelerated tests. One possible reason is that a larger amount of anticorrosive pigment may increase heterogeneity in the coating, creating more pathways and defects on the coating and making the increased inhibitor inefficient, as was observed in the accelerated tests. The

accelerated tests may also increase the leaching of the inhibitor and its concentration at the interface, but it has been shown that a higher concentration of vanadates does not always mean a greater inhibition but depends on the predominant speciation [42].

5. Conclusions

- HT-V (10%) primer may be considered a chromate alternative for slightly aggressive environments.
- HT-V (5%) offers good anticorrosive behavior in slightly and moderately aggressive environments, while HT-V (15%) shows poor behavior in the accelerated corrosion tests, due to the presence of defects and bad adhesion to the substrate, although it behaves well in short (1 year) natural exposure.
- In the very aggressive Kesternich test, a significant preponderance of zinc chromate over all the studied HT-V primers was observed. However, the high solubility of chromates leads to significant blistering in the condensing humidity test.

Acknowledgements

The authors gratefully acknowledge the financial support for this work from the Ministry of Science and Innovation of Spain (CICYT-MAT 2005-06261) and to *J. Guzmán* of *Productos Diez* for paint manufacture. J.M. Vega also acknowledges the PhD scholarship financed by CSIC-MICINN.

TABLE and FIGURE CAPTIONS

Table 1. Formulation of the studied alkyd paints, showing composition as %wt of components between brackets.

Table 2. Summary of results obtained in the accelerated corrosion tests.

Table 3. Summary of coating resistance (R_p, $\Omega*cm^2$) values from panels exposed in different accelerated corrosion tests (Table 2).

Table 4. Summary of phase angle value (θ) at low frequency (10 mHz) and capacitance (F/cm^2) obtained for the different primers after one year of exposure to Madrid and Aviles atmospheres.

Figure 1. Nyquist plots obtained during immersion in 0.1M Na_2SO_4 aqueous solution of 9.62 cm^2 paint samples after one year of exposure in the natural atmosphere of Madrid.

Figure 2. Nyquist plots obtained during immersion in 0.1M Na_2SO_4 aqueous solution of 9.62 cm^2 paint samples after one year of exposure in the natural atmosphere of Aviles.

Figure 3. Classic equivalent circuit for the metal/paint system.

Figure 4. Bode plots obtained during immersion in 0.1M Na_2SO_4 aqueous solution of 9.62 cm^2 paint samples after 168h of exposure in the condensing humidity test.

Figure 5 Adhesion results according to ISO 2409:1991 (E), where "0" means excellent adhesion and "5" very bad adhesion.

Figure 6. Bode plots obtained during immersion in 0.1M Na_2SO_4 aqueous solution of 9.62 cm^2 paint samples after 576h of exposure in the salt spray test.

Figure 7. Bode plots obtained during immersion in 0.1M Na_2SO_4 aqueous solution of 9.62 cm^2 paint samples after 1008h of exposure in the Kesternich test.

Figure 8. Appearance of the HT-V (15%) primer after 120h of exposure to the Kesternich test, showing significant delamination.

Table 1. Formulation of the studied alkyd paints, showing composition as %wt of components between brackets.

.

Designation	Binder	Anticorrosive Pigment	Others	Pigment Volume Concentration (PVC)
TiO_2 (25%)	Linseed-soybean oil modified alkyd resin (35.5)	None	TiO_2 (25), CaO (20)	38.3
$ZnCrO_4$ (10%)		$ZnCrO_4$ (10)	TiO_2 (20), CaO (15)	38.0
HT-V (5%)		HT-V (5)	TiO_2 (20), CaO (20)	39.4
HT-V (10%)		HT-V (10)	TiO_2 (20), CaO (15)	39.3
HT-V (15%)		HT-V (15)	TiO_2 (20), CaO (10)	39.3

Table 2. Summary of results obtained in the accelerated corrosion tests.

Designation	Condensing Humidity		Salt Spray		Kesternich (0.2 L)	
	Delamination at the Scribe (mm)	Blistering of the painted surface	Delamination at the Scribe (mm)	Blistering of the painted surface	Delamination at the Scribe (mm)	Blistering of the painted surface
	816 h	300 h	576 h	780 h	318 h	318 h
TiO_2 (25%)	0	7	0	9	0	9
$ZnCrO_4$ (10%)	0	5	0	9	0	9
HT-V (5%)	0	3	0	10	0	8
HT-V (10%)	0	7	0	9	4	9
HT-V (15%)	0	3	0	10	*	*

* Significant paint failure was observed at 120h (Figure 8).

Table 3. Summary of coating resistance (R_p, $\Omega*cm^2$) values from panels exposed in different accelerated corrosion tests (Table 2).

Designation	**Condensing Humidity** R_p ($\Omega*cm^2$)		**Salt Spray** R_p ($\Omega*cm^2$)		**Kesternich (0.2 L)** R_p ($\Omega*cm^2$)	
	168 h	**816 h**	**168 h**	**576 h**	**672 h**	**1008 h**
TiO_2 (25%)	$3.6\ 10^{+08}$	$2.5\ 10^{+09}$	$5.1\ 10^{+10}$	$1.5\ 10^{+11}$	$4.9\ 10^{+07}$	$9.8\ 10^{+08}$
$ZnCrO_4$(10%)	$1.3\ 10^{+09}$	$3.0\ 10^{+10}$	$1.0\ 10^{+11}$	$7.3\ 10^{+11}$	$4.9\ 10^{+10}$	$3.2\ 10^{+10}$
HT-V (5%)	$2.8\ 10^{+08}$	$9.2\ 10^{+08}$	$1.2\ 10^{+09}$	$9.8\ 10^{+09}$	$1.2\ 10^{+10}$	$2.9\ 10^{+07}$
HT-V (10%)	$2.8\ 10^{+06}$	$1.5\ 10^{+07}$	$6.9\ 10^{+11}$	$3.8\ 10^{+11}$	$8.9\ 10^{+09}$	$2.8\ 10^{+08}$
HT-V (15%)	$1.2\ 10^{+08}$	$3.8\ 10^{+08}$	$7.7\ 10^{+08}$	$4.5\ 10^{+09}$	*	*

* Significant paint failure was observed at 120h (Figure 8).

Table 4. Summary of phase angle value (θ) at low frequency (10 mHz) and capacitance (F/cm^2) obtained for the different primers after one year of exposure in Madrid and Aviles atmospheres.

Designation	Phase angle (θ) at 10 mHz		Capacitance (F/cm^2)	
	Madrid	**Aviles**	**Madrid**	**Aviles**
TiO_2 (25%)	-12	-17	$8.6\ 10^{-10}$	$1.0\ 10^{-09}$
$ZnCrO_4$ (10%)	-9	-81	$1.0\ 10^{-9}$	$1.3\ 10^{-10}$
HT-V (5%)	-60	-35	$6.4\ 10^{-10}$	$8.3\ 10^{-10}$
HT-V (10%)	-46	-77	$7.9\ 10^{-10}$	$4.5\ 10^{-10}$
HT-V (15%)	-70	-70	$9.2\ 10^{-10}$	$9.6\ 10^{-10}$

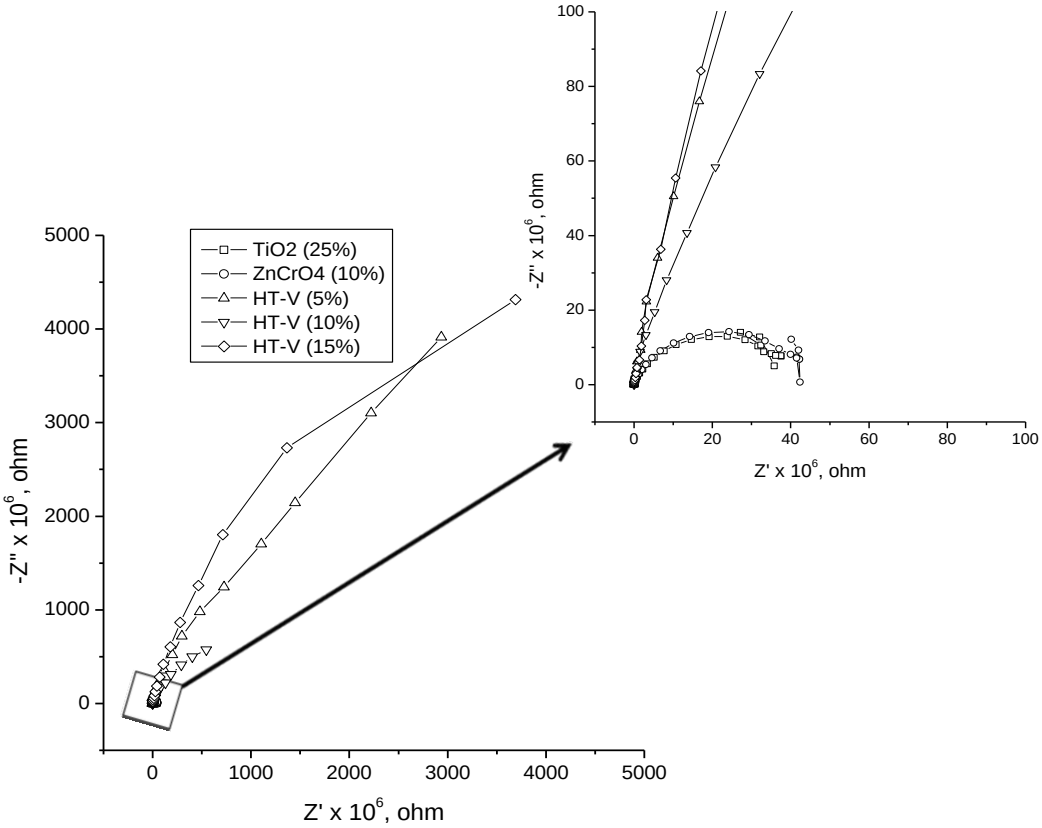

Figure 1. Nyquist plots obtained during immersion in 0.1M Na_2SO_4 aqueous solution of 9.62 cm^2 paint samples after one year of exposure in the natural atmosphere of Madrid.

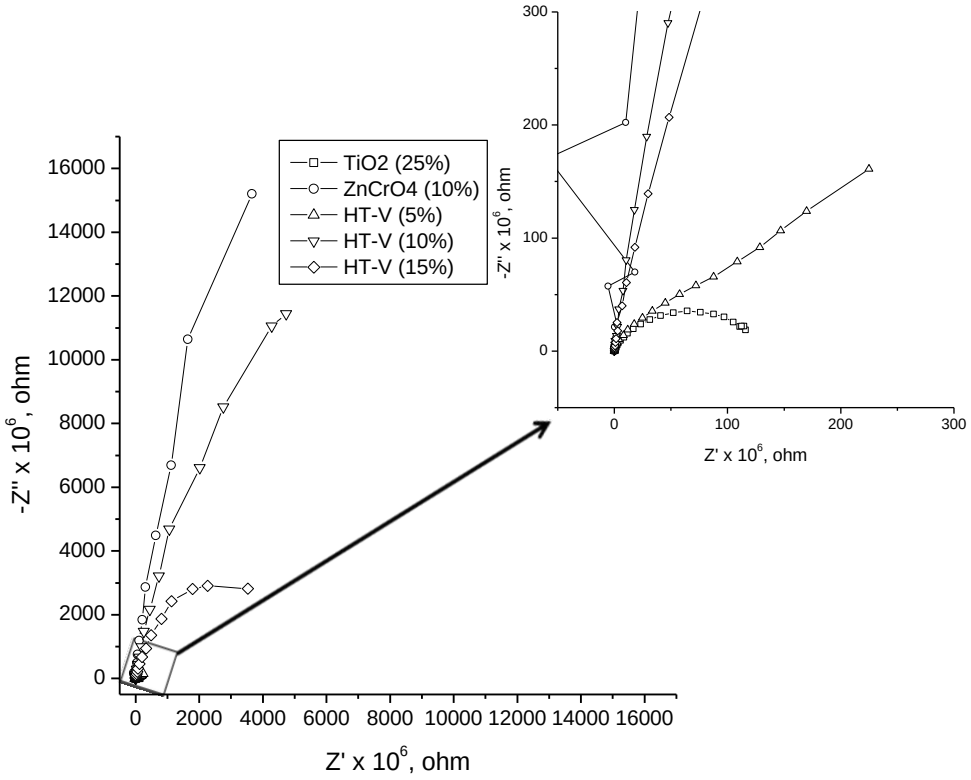

Figure 2. Nyquist plots obtained during immersion in 0.1M Na_2SO_4 aqueous solution of 9.62 cm^2 paint samples after one year of exposure in the natural atmosphere of Aviles.

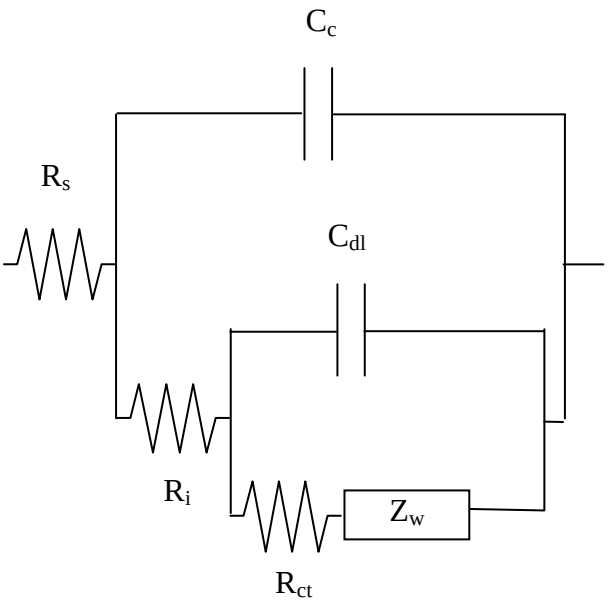

Figure 3. Classic equivalent circuit for the metal/paint system.

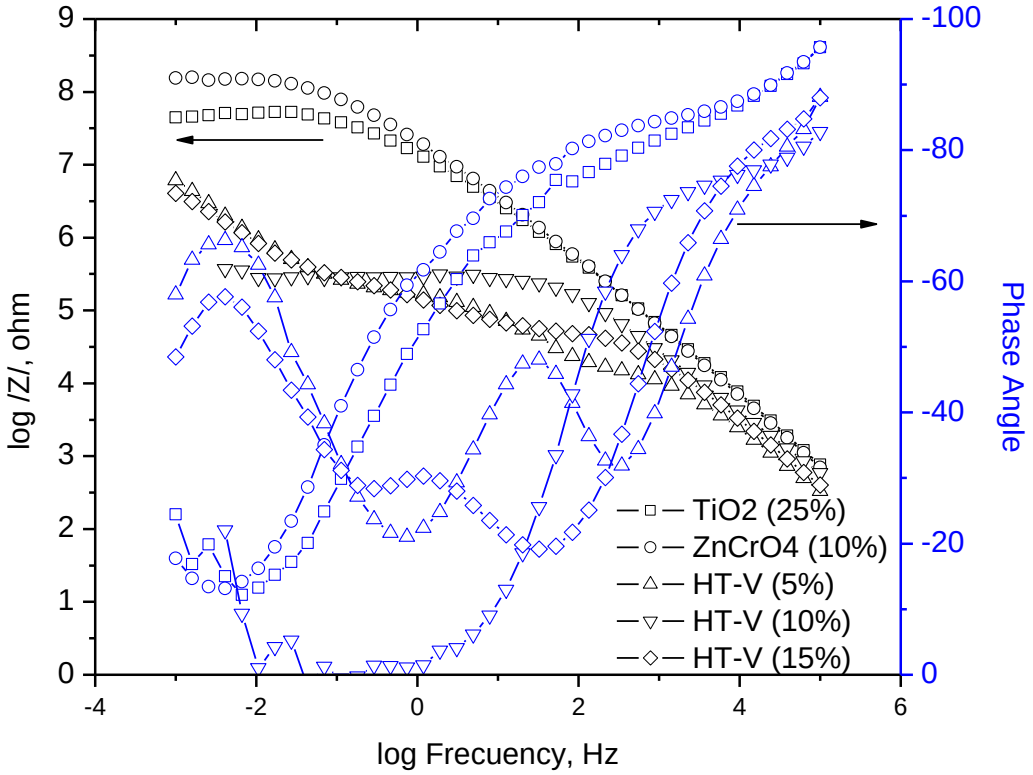

Figure 4. Bode plots obtained during immersion in 0.1M Na_2SO_4 aqueous solution of 9.62 cm^2 paint samples after 168h of exposure in the condensing humidity test.

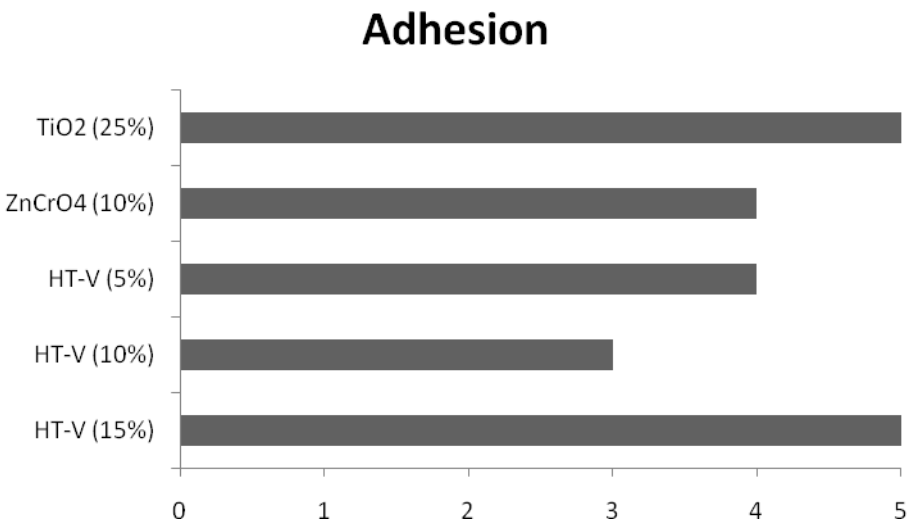

Figure 5 Adhesion results according to ISO 2409:1991 (E), where “0” means excellent adhesion and “5” very bad adhesion.

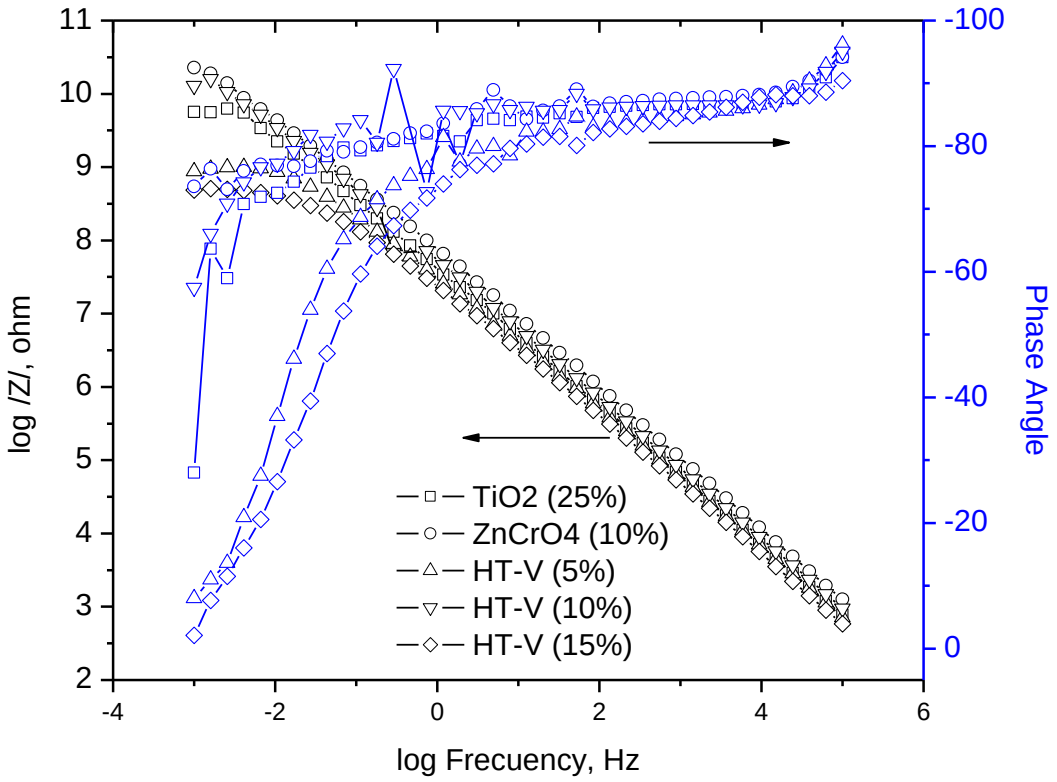

Figure 6. Bode plots obtained during immersion in 0.1M Na_2SO_4 aqueous solution of 9.62 cm^2 paint samples after 576h of exposure in the salt spray test.

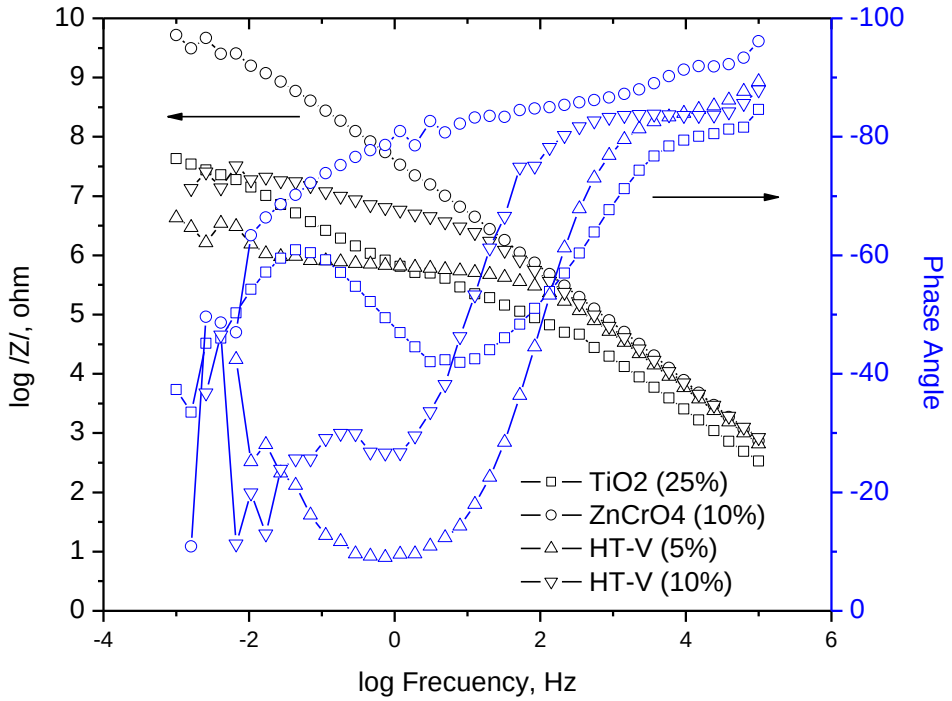

Figure 7. Bode plots obtained during immersion in 0.1M Na_2SO_4 aqueous solution of 9.62 cm^2 paint samples after 1008h of exposure in the Kesternich test.

Figure 8 Appearance of the HT-V (15%) primer after 120h of exposure to the Kesternich test, showing significant delamination.

References:

[1] F. L. Floyd, R. G. Groseclose, C. M. Frey, Journal of the Oil & Colour Chemists Association 66 (1983) 329-341.
[2] M. Kendig, M. Hon, Electrochemical and Solid State Letters 8 (2005) B10-B11.
[3] S. K. Poznyak, J. Tedim, L. M. Rodrigues, A. N. Salak, M. L. Zheludkevich, L. F. P. Dick, M. G. S. Ferreira, Acs Applied Materials & Interfaces 1 (2009) 2353-2362.
[4] Anne-Lise Troutier-Thuilliez, Christine Taviot-Guého, Joël Cellier, Horst Hintze-Bruening, Fabrice Leroux, Progress in Organic Coatings 64 (2009) 182-192.
[5] Horst Hintze-Bruening, Anne-Lise Troutier-Thuilliez, Fabrice Leroux, Progress in Organic Coatings 64 (2009) 193-204.
[6] F. Wong, R. G. Buchheit, Progress in Organic Coatings 51 (2004) 91-102.
[7] R. B. Leggat, S. A. Taylor, S. R. Taylor, Colloids and Surfaces a-Physicochemical and Engineering Aspects 210 (2002) 69-81.
[8] R. B. Leggat, S. A. Taylor, S. R. Taylor, Colloids and Surfaces a-Physicochemical and Engineering Aspects 210 (2002) 83-94.
[9] H. N. McMurray, G. Williams, Corrosion 60 (2004) 219-228.
[10] G. Williams, H. N. McMurray, Electrochemical and Solid State Letters 6 (2003) B9-B11.
[11] G. Williams, H. N. McMurray, Electrochemical and Solid State Letters 7 (2004) B13-B15.
[12] D. Álvarez, A. Collazo, M. Hernández, X. R. Nóvoa, C. Pérez, Progress in Organic Coatings 67 (2010) 152-160.
[13] J. K. Lin, J. Y. Uan, Corrosion Sci. 51 (2009) 1181-1188.
[14] Xiang Yu, Jun Wang, Milin Zhang, Piaoping Yang, Lihui Yang, Dianxue Cao, Junqing Li, Solid State Sciences 11 (2009) 376-381.
[15] Fazhi Zhang, Meng Sun, Sailong Xu, Lili Zhao, Bowen Zhang, Chemical Engineering Journal 141 (2008) 362-367.
[16] W. Zhang, R. G. Buchheit, Corrosion 58 (2002) 591-600.
[17] R. B. Leggat, W. Zhang, R. G. Buchheit, S. R. Taylor, Corrosion 58 (2002) 322-328.
[18] J. Wang, D. D. Li, X. Yu, X. Y. Jing, M. L. Zhang, Z. H. Jiang, Journal of Alloys and Compounds 494 (2010) 271-274.
[19] J. K. Lin, C. L. Hsia, J. Y. Uan, Scripta Materialia 56 (2007) 927-930.
[20] R. G. Buchheit, S. B. Mamidipally, P. Schmutz, H. Guan, Corrosion 58 (2002) 3-14.
[21] R. G. Buchheit, H. Guan, JCT Research 1 (2004) 277-290.
[22] Fazhi Zhang, Lili Zhao, Hongyun Chen, Sailong Xu, David G. Evans , Xue Duan, Angewandte Chemie International Edition 47 (2008) 2466-2469.
[23] X. X. Guo, S. L. Xu, L. L. Zhao, W. Lu, F. Z. Zhang, D. G. Evans, X. Duan, Langmuir 25 (2009) 9894-9897.
[24] S. P. V. Mahajanarn, R. G. Buchheit, Corrosion 64 (2008) 230-240.
[25] B. Chico, J. Simancas, J. M. Vega, N. Granizo, I. Diaz, D. de la Fuente, M. Morcillo, Progress in Organic Coatings 61 (2008) 283-290.
[26] M. L. Zheludkevich, S. K. Poznyak, L. M. Rodrigues, D. Raps, T. Hack, L. F. Dick, T. Nunes, M. G. S. Ferreira, Corrosion Sci. 52 (2010) 602-611.
[27] R. G. Buchheit, H. Guan, S. Mahajanam, F. Wong, Progress in Organic Coatings 47 (2003) 174-182.
[28] F. Kooli, W. Jones, Inorganic Chemistry 34 (1995) 6237-&.

[29] ISO 787-10, General methods of test for pigments and extenders -- Part 10: Determination of density -- Pyknometer method, Geneve, 1993.
[30] ISO 2409:1991: Paints and varnishes -- Cross-cut test, Geneve, 1991.
[31] ISO 6270-1, Paints and varnishes -- Determination of resistance to humidity -- Part 1: Continuous condensation, Geneve, 1998.
[32] ISO 9227, Corrosion tests in artificial atmospheres -- Salt spray tests, Geneve, 2006.
[33] ISO 3231, Paints and varnishes -- Determination of resistance to humid atmospheres containing sulfur dioxide, Geneve, 1993.
[34] ISO 9223, Corrosion of metals and alloys -- Corrosivity of atmospheres -- Classification, Geneve, 1992.
[35] ASTM 714D, Evaluating Degree of Blistering of Paints, ASTM, Philadelphia, 1987.
[36] J.D. Keane, J.A. Bruno, R.E.F. Weaver, Performance of alternate coatings in the environment, Steel Structure Painting Council (SSPC), Pittsburgh, 1979.
[37] S. Feliu, J. C. Galván, M. Morcillo, Progress in Organic Coatings 17 (1989) 143-153.
[38] S. Feliu, J. C. Galván, M. Morcillo, Corrosion Sci. 30 (1990) 989-998.
[39] J. C. Galván, S. Feliu, M. Morcillo, Progress in Organic Coatings 17 (1989) 135-142.
[40] N. Granizo, PhD Thesis, Universidad Alcalá de Henares, Madrid (2010)
[41] H. Corti, G. Baro, R. Fernandezprini, A. G. J. Maroto, Journal of the Oil & Colour Chemists Association 61 (1978) 75-78.
[42] K. D. Ralston, T. L. Young, R. G. Buchheit, Journal of The Electrochemical Society 156 (2009) C135-C146.